HHS Public Access

Author manuscript

Radiat Res. Author manuscript; available in PMC 2015 April 30.

Published in final edited form as:

Radiat Res. 2008 June ; 169(6): 607–614. doi:10.1667/RR1310.1.

Long-Term Dose Response of Trabecular Bone in Mice to Proton Radiation

Eric R. Bandstra[a], **Michael J. Pecaut**[b], **Erica R. Anderson**[a], **Jeffrey S. Willey**[a], **Francesco De Carlo**[c], **Stuart R. Stock**[d], **Daila S. Gridley**[b], **Gregory A. Nelson**[b], **Howard G. Levine**[e], and **Ted A. Bateman**[a,1]

[a]Department of Bioengineering, Clemson University, Clemson, South Carolina

[b]Department of Radiation, Loma Linda University and Medical Center, Loma Linda, California

[c]XOR, Advanced Photon Source, Argonne National Laboratory, Argonne, Illinois

[d]Department of Molecular Pharmacology and Biological Chemistry, Northwestern University Feinberg School of Medicine, Chicago, Illinois

[e]NASA Sustainable Systems Division, Kennedy Space Center, Florida

Abstract

Astronauts on exploratory missions will experience a complex environment, including microgravity and radiation. While the deleterious effects of unloading on bone are well established, fewer studies have focused on the effects of radiation. We previously demonstrated that 2 Gy of ionizing radiation has deleterious effects on trabecular bone in mice 4 months after exposure. The present study investigated the skeletal response after total doses of proton radiation that astronauts may be exposed to during a solar particle event. We exposed mice to 0.5, 1 or 2 Gy of whole-body proton radiation and killed them humanely 117 days later. Tibiae and femora were analyzed using microcomputed tomography, mechanical testing, mineral composition and quantitative histomorphometry. Relative to control mice, mice exposed to 2 Gy had significant differences in trabecular bone volume fraction (−20%), trabecular separation (+11%), and trabecular volumetric bone mineral density (−19%). Exposure to 1 Gy radiation induced a nonsignificant trend in trabecular bone volume fraction (−13%), while exposure to 0.5 Gy resulted in no differences. No response was detected in cortical bone. Further analysis of the 1-Gy mice using synchrotron microCT revealed a significantly lower trabecular bone volume fraction (−13%) than in control mice. Trabecular bone loss 4 months after exposure to 1 Gy highlights the importance of further examination of how space radiation affects bone.

INTRODUCTION

Bone loss as a result of microgravity exposure has been the subject of investigation for several years (1). Recently, volumetric quantitative computed tomography has been applied to allow for the resolution of differences in cortical and trabecular bone in astronauts (2, 3).

[1]Address for correspondence: 501 Rhodes Research Center, Clemson University, Clemson, SC 29631; bateman@clemson.edu.

Astronauts on the International Space Station (ISS) for 4.3–6.5-month missions had significant losses of cortical and trabecular bone in the vertebrae and proximal femur (3). Follow-up examinations of astronauts 1 and 5 years after space flight have revealed incomplete recovery of these deficits, including trabecular and cortical volumetric bone mineral density, estimated strength indices (4), and bone mineral (5). Markers of bone resorption in astronauts increased beginning early in flight, while markers for bone formation were unchanged during flight (6).

Exposure to ionizing radiation from solar and cosmic sources presents another challenge that astronauts will face during planned long-duration missions to the Moon or Mars (7). Previously, we demonstrated that a single 2-Gy exposure to several types of radiation (photons, protons and heavy ions) relevant to space flight has a profound negative effect on trabecular bone in mice (8). Exposure to high-LET and low-LET radiation had similar effects on the trabecular volume fraction (−29% to −39%) and connectivity density (−46% to −64%), with proton radiation resulting in reductions of −35% and −64%, respectively. A limited number of other studies have investigated bone loss using doses and types of radiation relevant to space flight (9–13). These studies have focused primarily on the effect of relatively high doses of carbon-ion radiation, with varied results. The response of bone and bone cells to proton radiation has not been studied adequately.

Gravitational and radiation environments will differ for lunar and Martian missions compared to current flights within low-Earth orbit. Astronauts traveling outside of the Earth's magnetic field will be exposed to higher doses of radiation. The primary sources of radiation beyond low-Earth orbit are galactic cosmic rays and solar particle events (SPEs). Galactic cosmic rays consist primarily of protons (~85%) (14). However, the remaining proportion (heavy ions) is particularly dangerous, because astronauts cannot be shielded from these highly energetic particles, which generally result in greater biological damage. While galactic cosmic rays are always present in space, the low particle fluence will result in a relatively small cumulative dose over a 6-month mission.

While cosmic rays result in a comparatively continuous low-dose-rate exposure, SPEs occur randomly and can deliver a higher dose, up to 2 Gy, in a short time (14–16). Although spacecraft shielding can effectively reduce radiation exposure, the warning provided by surveillance mechanisms may not allow for complete protection during extravehicular activities on the lunar surface (17). Even when protected by a mass of 5 g/cm^2 (e.g., 1.9 cm of aluminum or 5 cm of water), rare solar events such as those observed during August 1972 and October 1989 could deliver whole-body radiation doses approaching 2 Gy (18). Given the planned 6–8-month duration of lunar outpost missions, a dose of approximately 1 Gy proton radiation is a realistic possibility and should be considered in planning (19–21).

While our previous work demonstrated the negative effects of 2 Gy of radiation on mouse trabecular bone (8), lower doses have not been investigated. Although a 2-Gy dose is possible during a severe SPE, lower doses are more probable. The purpose of the present study was to examine the functional response of mouse bone 4 months after exposure to radiation relevant to space flight to determine a potential dose response. The results also provide a more thorough examination of cortical bone after irradiation. An understanding of

the doses that lead to changes in cortical and trabecular bone will allow for appropriate countermeasures to be developed and will facilitate a well-informed examination of radiation exposure combined with disuse.

MATERIALS AND METHODS

Animals

To mimic the study design used previously (8), 48 female C57BL/6J mice (Jackson Laboratory, Bar Harbor, ME) were shipped to Loma Linda University and acclimatized for 2 weeks under standard conditions. All protocols were approved by the appropriate Institutional Animal Care and Use Committees (Loma Linda University, Kennedy Space Center and Clemson University). Animals were grouped by weight to receive 0, 0.5, 1 or 2 Gy of proton radiation (n = 12/group) when 58 days old.

Irradiation

Immediately prior to irradiation, each mouse (irradiated and sham-irradiated) was placed individually in a rectangular plastic box (30 × 30 × 85 mm) with air holes as described previously (22). A maximum of six mice were irradiated simultaneously within a 20 × 20-cm field. Whole-body irradiation was performed using 250 MeV protons from the synchrotron accelerator housed at the Loma Linda University Medical Center as described previously (22, 23). Mice were irradiated at the entrance region of the Bragg curve with a dose rate of ~0.7 Gy/min. Protons were delivered in 0.3-s pulses every 2.2 s. Mice were irradiated behind a 400 × 400-mm^2 polystyrene phantom. Dose calibration was performed using a Markus parallel-plate ionization chamber (NIST traceable). The calibration method in ICRU Report 59 (24) was used to convert the ionization signal to dose in water. After the mice were irradiated, they were observed until they resumed normal posture and behavior. Three days after exposure, the mice were shipped to NASA Kennedy Space Center, where they were housed at the Space Life Sciences Animal Care Facility for the duration of the experiment.

Study End Point

As a fluorescent marker for bone mineralization, animals were given twice daily injections of calcein (10 mg/kg each injection, four total subcutaneous injections) at 34 and 33 days before they were killed humanely 117 days after irradiation. Multiple injections were used because of the age (and thus the low bone turnover) of the mice. Mice were anesthetized with isoflurance and exsanguinated by cardiac puncture, and then cervical dislocation was performed to ensure death. Left femora and tibiae were collected, cleaned of all non-osseous tissue, and measured for length. Left femora were allowed to air dry for 24 h and tibiae were stored in 70% ethanol. Right femora were collected and fixed in 10% neutral buffered formalin. Tissues were shipped to Clemson University for analysis.

Serum Analyses

At killing, samples of whole blood were collected by cardiac puncture and serum was separated. Markers of bone turnover present in the serum were measured using ELISA kits for osteocalcin (BT-470, Biomedical Technologies, Inc., Stoughton, MA) and TRAP5b (SB-

TR103, Immunodiagnostic Systems Inc., Fountain Hills, AZ). All procedures were performed according to the manufacturers' protocols.

Analysis of Bone Microarchitecture

Cortical and trabecular bone architecture was analyzed using microcomputed tomography (μCT20, Scanco Medical, Basserdorf, Switzerland) with an isotropic voxel size of 9 μm. Trabecular bone microarchitecture was scanned immediately distal to the growth plate in the proximal tibiae. Analysis of trabecular bone was performed on 100 slices (0.9 mm total), producing images for visual inspection and bone parameters. Bone morphometric parameters were quantified using Scanco software. Trabecular parameters included trabecular bone volume fraction (BV/TV), connectivity density (Conn.D), trabecular thickness (Tb.Th), trabecular number (Tb.N), trabecular separation (Tb.Sp), and trabecular volumetric bone mineral density (vBMD). Cortical bone analysis was performed at three sites: the femur third trochanter, the femur mid-diaphysis, and the tibial-fibular junction, with 30 slices (approximately 0.3 mm) selected at each site. Bone volume (BV), cortical porosity (Ct.Po), and polar moment of inertia (pMOI) were calculated from these sections.

To further clarify data obtained near an apparent dose threshold beyond which exposure results in impaired bone volume and architecture, synchrotron microCT analysis was performed to improve resolution and reduce variability. A subset of the control and 1-Gy groups were scanned using station 2-BM of APS (Advanced Photon Source, Argonne National Laboratory, Argonne, IL). A monochromatic beam (photon energy of 17 keV) and a 2Kx2K element CCD camera coupled (by a Zeiss AXIO-PLAN 2.5× neofluar lens) to a single-crystal $CdWO_4$ scintillator were used. Views were recorded every 0.125° from 0° to 180° and were normalized for detector and beam nonuniformities; the samples were reconstructed on a 2048 × 2048-grid of isotropic 2.66-μm voxels. Additional details are presented elsewhere (24). Scans were performed to include the portion of the proximal tibia analyzed previously using the laboratory scanner. Files were converted to binary format and imported into the Scanco-supported server for analysis. The images were compared to the previous scans from the Scanco μCT20 to ensure that analysis of the trabecular bone was performed at a similar location in both cases. The Scanco software was used to determine trabecular volume fraction.

Mechanical Testing

Left (air-dried) femora were rehydrated in PBS for 90 min prior to evaluation to simulate *in vivo* properties (25). Three-point bending tests were performed using an Instron 5582 (BlueHill 2 software, Instron Corp., Norwood, MA). Femora were tested to failure with a 9-mm span length and a deflection rate of 5 mm/min. All bones were tested in the same orientation; the single-point load was applied mid-diaphysis on the posterior surface. The maximal force (N) and deflection (mm) were measured for all mechanically tested bones. These two properties were also determined at the elastic limit (P_e, δ_e) and the failure point. Stiffness (N/mm) was calculated from P_e/δ_e.

Mineral Composition

Analysis of mineral content was performed on fractured femora. Prior to analysis, the enlarged ends of the femora were separated where distal and proximal metaphyses join the diaphysis. Mineral content data were obtained separately from bone ends and diaphysis. A properly calibrated microbalance (Mettler Toledo UMT2; Columbus, OH) was used for all measurements. Dry mass was measured after the bones were heated to 105°C for 24 h. Mineral mass was measured after the bones had been ashed by baking at 800°C for another 24 h. The percent mineralization was calculated as mineral mass/dry mass × 100.

Quantitative Histomorphometry

Right (fixed) femora were allowed to air-dry and then were embedded with non-infiltrating Epo-Kwick epoxy (Buehler Ltd., Lake Bluff, IL). The formed disks were sectioned with a low-speed saw (Buehler, 12.7 × 0.5-mm diamond blade) at the mid-diaphysis of the femur. These sections were wheel-polished to a flat, smooth surface using 600-, 800- and 1200-grit carbide paper followed by polishing with a cloth impregnated with 6 μm diamond paste. This allowed micrographs to be taken of the bone cross sections at 50× magnification under UV light (400 nm) with an FS filter. Quantitative histomorphometric analysis was performed using these photographs and SigmaScan Pro software (SPSS, San Rafael, CA).

Analysis of the photographs was used to calculate bone formation rate (BFR) for both the periosteal (Ps.BFR) and endocortical (Ec.BFR) surfaces (26). Bone formation rate was calculated as the product of mineralized surface (MS) and mineral apposition rate (MAR). Mineralized surface was measured as the length of the calcein label. Mineral apposition rate was measured as the distance between the calcein label and the cortical perimeter divided by the time between label administration and tissue harvesting (34 days).

Statistics

Statistical analysis of results was completed using SigmaStat software v3.5 (Systat Software Inc., San Jose, CA). Comparisons were made using a one-way analysis of variance (ANOVA) with a Student-Newman-Keuls *post hoc* test to reveal significance between groups. The only exception was the synchrotron microCT data, which was compared using a *t* test. Statistical significance was set at $P < 0.05$. Because our goal was to establish a dose threshold for bone response to proton radiation, differences representing nonsignificant trends ($P < 0.1$) in bone microarchitectural parameters are presented as data of interest. All data are presented as means ± SD.

RESULTS

MicroCT Analysis of Trabecular and Cortical Bone

MicroCT analysis of trabecular bone within the proximal tibia using the laboratory scanner revealed significant differences in animals exposed to 2 Gy of proton radiation (compared to control animals), which included a 20% smaller trabecular volume fraction ($P = 0.011$; Fig. 1), an 11% greater trabecular separation ($P = 0.046$; Fig. 1), a 19% smaller volumetric bone mineral density ($P = 0.025$; Fig. 1), and a nonsignificant trend in trabecular number (+9%; $P = 0.093$; Table 1). Mice exposed to 1 Gy had no significant differences in microarchitecture,

including volumetric bone mineral density and trabecular number ($P > 0.1$; Fig. 1, Table 1). However, these mice did exhibit non-significant trends relative to control in trabecular volume fraction (−13%; $P = 0.062$; Fig. 1) and trabecular separation (+9%; $P = 0.094$; Fig. 1). Mice exposed to 0.5 Gy had no significant differences in trabecular bone parameters compared with control mice, including trabecular volume fraction, trabecular separation, trabecular number, and volumetric bone mineral density ($P > 0.1$; Fig. 1, Table 1). Radiation treatment did not result in different values for polar moment of inertia, cortical volume or cortical porosity between groups (Table 2).

Subsequent synchrotron microCT analysis of the trabecular bone in the proximal tibia of the control and 1-Gy groups revealed a significant 13% smaller trabecular volume fraction in irradiated animals ($P = 0.041$; Fig. 1).

Growth Parameters

Animal weight in all groups was similar at the initiation of the study ($P > 0.05$; Table 3). At tissue collection, no between-group differences were observed in animal weight, tibial length or femoral length ($P > 0.05$; Table 3).

Additional Bone Assays

No differences in mechanical strength (force or deflection) were observed in the irradiated animals compared to controls or other treatment groups ($P > 0.05$; Table 4). Likewise, no between-group differences in serum osteocalcin or TRAP5b concentration (Table 5), bone formation rate, and mineral composition were observed (Table 6) ($P > 0.05$).

DISCUSSION

The results of this study confirm that trabecular bone loss occurs after exposure to 2 Gy of proton radiation (8). In addition, we found that a 1-Gy dose of proton radiation has detectable negative effects on trabecular volume fraction 4 months after exposure. This is an important finding with respect to future lunar outpost missions, which are planned to last 6–8 months. While exposure to 2 Gy radiation is possible on these missions, exposure to 1 Gy is much more likely and should be considered in mission planning (19–21).

In the bones harvested 4 months after proton irradiation, the dose threshold resulting in trabecular deterioration appeared to be between 0.5 and 1 Gy. It is possible that bone loss did occur at the lower dose (0.5 Gy) but that the loss was recovered by the end of the 4-month experiment. The lack of an observed difference in bone turnover markers between groups, combined with similar bone formation rates, suggests that bone turnover has stabilized 4 months after irradiation. Lower trabecular volume fraction was observed in the mice exposed to 1 and 2 Gy of protons, supporting the contention that bone loss occurred earlier than 4 months and did not recover. This lower bone volume suggests that the degree of loss may be permanent, although examination at later times will be necessary to draw any definitive conclusion.

Our data do not indicate whether decreased bone formation or increased bone resorption caused the reduction in trabecular bone after irradiation. Reduced formation could contribute

to the reduced bone volume we found. While most of the studies investigating radiation effects on osteoblasts use much higher doses than we used, it has been demonstrated that 2 Gy of X rays results in reduced numbers of pre-osteoblasts and inhibits their differentiation *in vitro* (27). Relatively few studies have examined osteoclasts (and changes in bone resorption) after irradiation (13, 28, 29). None of these studies have documented significant increases in osteoclast numbers after irradiation, nor has a change in the expression of some important regulators of osteoclast activity [namely receptor activator of NF-κB ligand (RANKL) and osteoprotegerin (OPG)] been documented relative to nonirradiated controls from mouse bone marrow cultured with 2 Gy carbon-ion- and γ-irradiated pre-osteoblasts (12). A time-course examination focusing on earlier points is required to define the contribution of formation and resorption to the change in bone.

Bone loss after irradiation is important in the context of the known atrophy of bone that occurs as a result of exposure to microgravity (3). Radiation thus represents another potential skeletal challenge astronauts must face in the space-flight environment. It is unclear and unstudied how the combination of these challenges can affect the quantity and architecture of bone; thus one can only speculate as to the resulting effects and association. The threshold of radiation-induced bone loss may change when combined with unloading. Also, the combined effect of unloading and radiation may not be additive, given the substantial effect of unloading on bone status. If the effects are synergistic, the possibility of both mission-critical and post-flight fractures could represent a risk to astronauts.

The absence of an effect of proton radiation on cortical bone parameters in the present study is in agreement with previous findings by our group [(8); N. D. Travis *et al.*, unpublished observations]. We investigated various parameters of strength, composition and formation in cortical bone; the results confirmed that bone loss after proton irradiation is specific to trabecular bone at moderate doses. Other studies investigating cortical bone after irradiation have found changes in cortical bone strength and porosity after very high doses (30, 31). However, fractionation of high doses mitigated changes in fracture strength (31), suggesting that lower or fractionated doses of radiation may not affect cortical bone.

An important consideration in the present study is that, to match the design of the previous study, the mice were 2 months old at irradiation. At this age, the mice were still growing and the skeletal system was not mature (32, 33). However, the similarities in animal weight and both femoral and tibial lengths in all test groups indicate that overall growth rates after irradiation were not grossly affected. Additionally, while animal weight, long-bone length, and cortical bone volume continue to increase through 4–6 months of age, trabecular bone volume fraction in C57BL/6J mice decreases after 2 months of age (32, 33). Therefore, the mice in this study were irradiated after the maximal trabecular volume fraction was achieved. Radiation-induced changes in bone growth might not translate into a reduced trabecular volume fraction. While these considerations indicate that overall changes in growth did not lead to the lesser trabecular volume fraction in irradiated mice, it is possible that some of the present bone loss could be attributed to altered conversion of growth cartilage to bony trabeculae. In addition, the higher bone formation and resorption rates in growing animals may affect how these animals respond to radiation. Thus, since astronauts

will be fully mature, it follows that older, skeletally mature animals should be studied in the future.

Although the age at exposure, strain and sex of mice, and duration of the experiment were identical to the conditions of our previous experiment with 2 Gy protons, the mice in the previous study had a greater degree of bone loss than those in the current study (35% compared to 20%) (8). Another notable difference between the studies was the significantly lower endogenous trabecular volume fraction in the nonirradiated mice (4% compared to 12%). The mice in this study clearly had less trabecular bone, possibly because the mice were obtained from different vendors (Jackson Laboratory and Charles River). This lower trabecular volume in the nonirradiated control mice is a characteristic that may provide insight into this difference in the amount of trabecular bone lost in the irradiated animals. For example, in osteoporosis models such as ovariectomy, it has been demonstrated that strains of mice with higher bone density lose proportionally greater amounts of trabecular bone (34). Though the genotype of the different strains likely contributed to the observed differences, the phenotype itself could influence the response. It is possible that the different responses in the studies is due to the greater endogenous bone mass of the mice in the previous study. Future studies should use various strains of mice to explore this potential phenotypic effect. In addition, animals such as rats that have more trabecular bone may prove to be good models for understanding the effects of radiation on bone.

Few studies have been performed examining the effects of increased spatial resolution and decreased voxel size available using synchrotron radiation microCT compared to conventional microCT. In the present study, trabecular volume fraction values obtained using synchrotron microCT were slightly lower than those for conventional microCT. However, the corresponding standard deviations were proportionally smaller, accounting for the significance even with the same percentage difference in trabecular volume fraction relative to control. Previous results have shown minimal effects of measured trabecular volume fraction with synchrotron radiation compared to conventional microCT (35, 36). These investigations have been performed on human samples with a trabecular bone thickness of the order of 100 μm, while the mice in the present study had values of approximately 50 μm. It is possible that the decrease in trabecular bone thickness would make the decreased voxel size have more influence on observed trabecular volume fraction. Previous examinations comparing synchrotron radiation and conventional microCT in animals have not presented quantitative results and thus do not allow for comparison (37).

The radiation used in the present study was acute, mono-energetic, proton radiation. However, radiation from an SPE will have a wide energy range and will be delivered over hours to days, not over minutes (14). In addition, many other types of radiation will be present in space from galactic cosmic rays. To fully understand the effects of radiation, more complex models of space radiation must be studied and combined with ground-based, modeled microgravity.

This study confirms a loss of trabecular bone in mice exposed to a 2-Gy dose of proton radiation and further demonstrates volumetric loss of bone with a 1-Gy dose of radiation 4 months after exposure. Trabecular bone is an important contributor to bone strength (38,

39). Because reduced bone strength indices have been estimated from the atrophied bones of astronauts returning from microgravity (3, 4), the loss of trabecular bone in response to radiation may further contribute to a decline in bone strength. The group of mice exposed to 0.5 Gy did not experience any differences in skeletal parameters; however, the absence of differences in bone turnover markers in the affected groups suggests that 4 months is a late time and that earlier periods need to be examined. It was confirmed that at this relatively late period after exposure, cortical bone volume and quality were not different from those of control mice, suggesting that the response may be trabecular-specific. As discussed, further study is needed to characterize this phenomenon. Future investigations should aim to increase understanding of the effects of moderate radiation doses on bone-forming and bone-resorbing cells. In the context of the known negative effects of microgravity on the skeletal system, additional bone loss from space radiation may result in mission-critical amounts of bone loss on exploratory missions to the Moon and Mars.

Acknowledgments

The authors would like to thank Brian Tieman for his work on the conversion of the APS data. In addition, the support of Ramona Bober, April Spinale and Kimberly Anderson at the Kennedy Space Center Space Life Sciences Laboratory is greatly appreciated. The editorial and formatting assistance of Jenny Bourne is greatly valued. The authors would also like to thank all members of the Osteoporosis Biomechanics Laboratory. This work was funded by the National Space Biomedical Research Institute through NASA NCC 9-58, BioServe Space Technologies through NASA NCC8-242, and the South Carolina Space Grant Consortium/NASA EPSCoR and was supported in part by NASA Cooperative Agreement NCC9-79 to GAN, Radiobiology Program, Loma Linda University. Use of the Advanced Photon Source was supported by the U.S. Department of Energy, Office of Science, Office of Basic Energy Sciences, under Contract No. DE-AC02-06CH11357. Fellowship support (ERB) provided by the South Carolina Space Grant Consortium and NASA Kennedy Space Center. This work was supported in part by an unrestricted grant from Procter & Gamble Pharmaceuticals.

References

1. Rambaut PC, Johnston RS. Prolonged weightlessness and calcium loss in man. Acta Astronaut. 1979; 6:1113–1122. [PubMed: 11883480]
2. Vico L, Collet P, Guignandon A, Lafage-Proust MH, Thomas T, Rehaillia M, Alexandre C. Effects of long-term microgravity exposure on cancellous and cortical weight-bearing bones of cosmonauts. Lancet. 2000; 355:1607–1611. [PubMed: 10821365]
3. Lang T, LeBlanc A, Evans H, Lu Y, Genant H, Yu A. Cortical and trabecular bone mineral loss from the spine and hip in long-duration spaceflight. J Bone Miner Res. 2004; 19:1006–1012. [PubMed: 15125798]
4. Lang TF, Leblanc AD, Evans HJ, Lu Y. Adaptation of the proximal femur to skeletal reloading after long-duration spaceflight. J Bone Miner Res. 2006; 21:1224–1230. [PubMed: 16869720]
5. Tilton FE, Degioanni JJ, Schneider VS. Long-term follow-up of Skylab bone demineralization. Aviat Space Environ Med. 1980; 51:1209–1213. [PubMed: 7213266]
6. Smith SM, Wastney ME, O'Brien KO, Morukov BV, Larina IM, Abrams SA, Davis-Street JE, Oganov V, Shackelford LC. Bone markers, calcium metabolism, and calcium kinetics during extended-duration space flight on the Mir space station. J Bone Miner Res. 2005; 20:208–218. [PubMed: 15647814]
7. NASA. A Roadmap for the Robotic and Human Exploration of Mars. NASA; Washington, DC: 2005.
8. Hamilton SA, Pecaut MJ, Gridley DS, Travis ND, Bandstra ER, Willey JS, Nelson GA, Bateman TA. A murine model for bone loss from therapeutic and space-relevant sources of radiation. J Appl Physiol. 2006; 101:789–793. [PubMed: 16741258]
9. Fukuda S, Iida H. Effects of clinostat-microgravity and heavy-particle radiation on bone and calcium metabolism in rats. J Jpn Soc Bone Morphom. 1999; 9:35–44.

10. Fukuda S, Iida H, Yan X. Preventive effects of running exercise on bones in heavy ion particle irradiated rats. J Radiat Res (Tokyo). 2002; 43(Suppl):S233–S238. [PubMed: 12793765]
11. Sawajiri M, Mizoe J. Changes in bone volume after irradiation with carbon ions. Radiat Environ Biophys. 2003; 42:101–106. [PubMed: 12768291]
12. Sawajiri M, Nomura Y, Bhawal UK, Nishikiori R, Okazaki M, Mizoe J, Tanimoto K. Different effects of carbon ion and gamma-irradiation on expression of receptor activator of NF-κB ligand in MC3T3-E1 osteoblast cells. Bull Exp Biol Med. 2006; 142:618–624. [PubMed: 17415477]
13. Sawajiri M, Mizoe J, Tanimoto K. Changes in osteoclasts after irradiation with carbon ion particles. Radiat Environ Biophys. 2003; 42:219–223. [PubMed: 13680258]
14. Benton ER, Benton EV. Space radiation dosimetry in low-Earth orbit and beyond. Nucl Instrum Methods Phys Res B. 2001; 184:255–294. [PubMed: 11863032]
15. Blakely EA. Biological effects of cosmic radiation: deterministic and stochastic. Health Phys. 2000; 79:495–506. [PubMed: 11045523]
16. Stephens DL Jr, Townsend LW, Hoff JL. Interplanetary crew dose estimates for worst case solar particle events based on historical data for the Carrington flare of 1859. Acta Astronaut. 2005; 56:969–974. [PubMed: 15835055]
17. Task Group on the Biological Effects of Space Radiation, Space Studies Board, Commission on Physical Sciences, Mathematics, and Applications, National Research Council. Radiation Hazards to Crews of Interplanetary Missions: Biological Issues and Research Strategies. National Academy Press; Washington, DC: 1996. p. 13-34.
18. Parsons JL, Townsend LW. Interplanetary crew dose rates for the August 1972 solar particle event. Radiat Res. 2000; 153:729–733. [PubMed: 10825747]
19. Cucinotta FA, Wu H, Shavers MR, George K. Radiation dosimetry and biophysical models of space radiation effects. Gravit Space Biol Bull. 2003; 16:11–18. [PubMed: 12959127]
20. Ohnishi K, Ohnishi T. The biological effects of space radiation during long stays in space. Biol Sci Space. 2004; 18:201–205. [PubMed: 15858386]
21. Cucinotta FA, Durante M. Cancer risk from exposure to galactic cosmic rays: implications for space exploration by human beings. Lancet Oncol. 2006; 7:431–435. [PubMed: 16648048]
22. Gridley DS, Pecaut MJ, Dutta-Roy R, Nelson GA. Dose and dose rate effects of whole-body proton irradiation on leukocyte populations and lymphoid organs: part I. Immunol Lett. 2002; 80:55–66. [PubMed: 11716966]
23. Gridley DS, Pecaut MJ, Miller GM, Moyers MF, Nelson GA. Dose and dose rate effects of whole-body gamma-irradiation: II. Hematological variables and cytokines. In Vivo. 2001; 15:209–216. [PubMed: 11491015]
24. ICRU. Clinical Proton Dosimetry Part 1: Beam Production, Beam Delivery and Measurement of Absorbed Dose. International Commission on Radiation Units and Measurements; Bethesda, MD: 1998. Report 59
25. Wang Y, De Carlo F, Mancini DC, McNulty I, Tieman B, Bresnahan J, Foster I, Insley J, Lane P, Thiebaux M. A high-throughput x-ray microtomography system at the Advanced Photon Source. Rev Sci Instrum. 2001; 72:2062–2068.
26. Broz JJ, Simske SJ, Greenberg AR, Luttges MW. Effects of rehydration state on the flexural properties of whole mouse long bones. J Biomech Eng. 1993; 115:447–449. [PubMed: 8309241]
27. Parfitt AM, Drezner MK, Glorieux FH, Kanis JA, Malluche H, Meunier PJ, Ott SM, Recker RR. Bone histomorphometry: standardization of nomenclature, symbols, and units. Report of the ASBMR Histomorphometry Nomenclature Committee. J Bone Miner Res. 1987; 2:595–610. [PubMed: 3455637]
28. Sakurai T, Sawada Y, Yoshimoto M, Kawai M, Miyakoshi J. Radiation-induced reduction of osteoblast differentiation in C2C12 cells. J Radiat Res (Tokyo). 2007; 48:515–521. [PubMed: 17928745]
29. Goblirsch M, Lynch C, Mathews W, Manivel JC, Mantyh PW, Clohisy DR. Radiation treatment decreases bone cancer pain through direct effect on tumor cells. Radiat Res. 2005; 164:400–408. [PubMed: 16187742]

30. Vit JP, Ohara PT, Tien DA, Fike JR, Eikmeier L, Beitz A, Wilcox GL, Jasmin L. The analgesic effect of low dose focal irradiation in a mouse model of bone cancer is associated with spinal changes in neuro-mediators of nociception. Pain. 2006; 120:188–201. [PubMed: 16360279]
31. Sugimoto M, Takahashi S, Toguchida J, Kotoura Y, Shibamoto Y, Yamamuro T. Changes in bone after high-dose irradiation. Biomechanics and histomorphology. J Bone Joint Surg Br. 1991; 73:492–497. [PubMed: 1670456]
32. Nyaruba MM, Yamamoto I, Kimura H, Morita R. Bone fragility induced by X-ray irradiation in relation to cortical bone-mineral content. Acta Radiol. 1998; 39:43–46. [PubMed: 9498868]
33. Halloran BP, Ferguson VL, Simske SJ, Burghardt A, Venton LL, Majumdar S. Changes in bone structure and mass with advancing age in the male C57BL/6J mouse. J Bone Miner Res. 2002; 17:1044–1050. [PubMed: 12054159]
34. Glatt V, Canalis E, Stadmeyer L, Bouxsein ML. Age-related changes in trabecular architecture differ in female and male C57BL/6J mice. J Bone Miner Res. 2007; 22:1197–1207. [PubMed: 17488199]
35. Bouxsein ML, Myers KS, Shultz KL, Donahue LR, Rosen CJ, Beamer WG. Ovariectomy-induced bone loss varies among inbred strains of mice. J Bone Miner Res. 2005; 20:1085–1092. [PubMed: 15940361]
36. Peyrin F, Salome M, Cloetens P, Laval-Jeantet AM, Ritman E, Ruegsegger P. Micro-CT examinations of trabecular bone samples at different resolutions: 14, 7 and 2 micron level. Technol Health Care. 1998; 6:391–401. [PubMed: 10100941]
37. Chappard C, Basillais A, Benhamou L, Bonassie A, Brunet-Imbault B, Bonnet N, Peyrin F. Comparison of synchrotron radiation and conventional x-ray microcomputed tomography for assessing trabecular bone microarchitecture of human femoral heads. Med Phys. 2006; 33:3568–3577. [PubMed: 17022253]
38. Ito M, Ejiri S, Jinnai H, Kono J, Ikeda S, Nishida A, Uesugi K, Yagi N, Tanaka M, Hayashi K. Bone structure and mineralization demonstrated using synchrotron radiation computed tomography (SR-CT) in animal models: preliminary findings. J Bone Miner Metab. 2003; 21:287–293. [PubMed: 12928829]
39. Borah B, Dufresne TE, Chmielewski PA, Gross GJ, Prenger MC, Phipps RJ. Risedronate preserves trabecular architecture and increases bone strength in vertebra of ovariectomized minipigs as measured by three-dimensional microcomputed tomography. J Bone Miner Res. 2002; 17:1139–1147. [PubMed: 12096826]
40. Guo XE, Kim CH. Mechanical consequence of trabecular bone loss and its treatment: a three-dimensional model simulation. Bone. 2002; 30:404–411. [PubMed: 11856649]

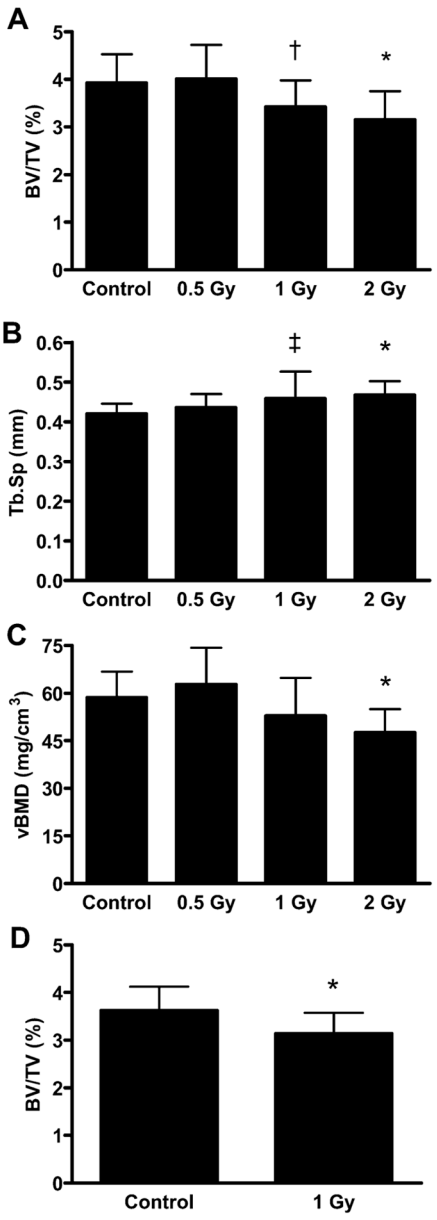

FIG. 1.

Microcomputed tomography parameters in the proximal tibiae including (panel A) trabecular volume fraction (BV/TV), (panel B) trabecular spacing (Tb.Sp), and (panel C) trabecular volumetric bone mineral density (vBMD) determined using a Scanco μCT20 and (panel D) trabecular volume fraction (BV/TV) as calculated from synchrotron microCT. *Significant difference from control ($P < 0.05$). †Trend toward difference from control ($P = 0.062$). ‡Trend toward difference from control ($P = 0.094$).

TABLE 1

Microcomputed Tomography Parameters for Trabecular Bone

	Conn.D (1/mm^3)	Tb.N (1/mm^3)	Tb.Th (μm)
Control	5.38 (1.69)	2.42 (0.16)	51.1 (5.4)
0.5 Gy	5.40 (2.99)	2.31 (0.16)	52.6 (3.7)
1 Gy	5.92 (3.13)	2.27 (0.36)	48.4 (3.9)
2 Gy	4.98 (1.97)	2.20 (0.16)[a]	52.3 (2.3)

Notes. Conn.D, connectivity density; Tb.N, trabecular number; Tb.Th, trabecular thickness. Data reported as mean (SD).

[a] Nonsignificant trend compared to control ($P = 0.093$).

TABLE 2

Microcomputed Tomography Parameters for Cortical Bone

	Tibal-fibular junction			Femur diaphysis			Femur trochanter	
	Ct.Po (%)	**BV (mm^3)**	**pMOI (mm^4)**	**Ct.Po (%)**	**BV (mm^3)**	**pMOI (mm^4)**	**Ct.Po (%)**	**BV (mm^3)**
Control	7.78 (0.37)	0.153 (0.009)	0.116 (0.010)	9.97 (0.42)	0.189 (0.008)	0.308 (0.026)	12.37 (1.48)	0.247 (0.011)
0.5 Gy	7.79 (0.46)	0.148 (0.008)	0.109 (0.009)	9.94 (0.34)	0.191 (0.008)	0.315 (0.026)	12.87 (1.27)	0.250 (0.009)
1 Gy	7.79 (0.61)	0.152 (0.010)	0.116 (0.011)	10.29 (0.55)	0.186 (0.011)	0.311 (0.033)	13.32 (1.78)	0.248 (0.013)
2 Gy	7.60 (0.35)	0.150 (0.008)	0.108 (0.008)	10.28 (0.47)	0.184 (0.010)	0.309 (0.033)	13.57 (1.57)	0.244 (0.013)

Notes. Ct.Po, cortical porosity; BV, bone volume; pMOI, polar moment of inertia. Data reported as mean (SD).

TABLE 3

Animal Masses, Tibia Lengths and Femur Lengths

	Initial animal mass (g)	Final animal mass (g)	Tibia (mm)	Femur (mm)
Control	18.1 (0.9)	22.8 (2.1)	17.6 (0.2)	15.3 (0.3)
0.5 Gy	18.3 (0.7)	23.6 (2.3)	17.5 (0.4)	15.3 (0.3)
1 Gy	18.3 (0.7)	23.5 (3.0)	17.5 (0.2)	15.3 (0.3)
2 Gy	18.4 (0.6)	24.2 (2.9)	17.5 (0.3)	15.3 (0.2)

Note. Data reported as means (SD).

TABLE 4

Mechanical Properties of Mouse Bone after Irradiation

		Force (N)			Deflection (mm)		
	Stiffness (N/mm)	**Elastic**	**Maximum**	**Fracture**	**Elastic**	**Maximum**	**Fracture**
Control	39.3 (5.9)	10.5 (1.9)	12.7 (2.1)	5.59 (1.41)	0.268 (0.041)	0.408 (0.029)	0.756 (0.193)
0.5 Gy	38.9 (10.2)	10.0 (2.8)	12.1 (3.1)	6.48 (2.67)	0.288 (0.152)	0.427 (0.118)	0.851 (0.326)
1 Gy	41.3 (5.7)	10.3 (1.4)	12.9 (2.0)	6.76 (1.77)	0.254 (0.050)	0.399 (0.052)	0.791 (0.291)
2 Gy	38.0 (6.1)	9.4 (1.4)	11.6 (1.9)	6.93 (2.27)	0.259 (0.081)	0.404 (0.061)	0.708 (0.229)

Note. Data reported as mean (SD).

TABLE 5

Serum Markers of Bone Turnover 4 Months after Irradiation

	TRAP5b (U/liter)	Osteocalcin (ng/ml)
Control	2.69 (0.50)	15.3 (4.3)
0.5 Gy	2.54 (0.47)	14.7 (3.1)
1 Gy	2.46 (0.57)	15.2 (4.3)
2 Gy	2.75 (0.26)	12.9 (3.6)

Note. Data reported as mean (SD).

TABLE 6

Histomorphometry and Percent Mineralization

	Histomorphometry		Percent mineralization		
	Ps.BFR (μm²/day)	**Ec.BFR (μm²/day)**	**Total**	**Bone end**	**Diaphysis**
Control	1870 (210)	641 (265)	59.7 (1.6)	56.5 (1.6)	65.3 (2.4)
0.5 Gy	1970 (310)	516 (320)	58.9 (2.2)	55.4 (2.9)	65.2 (2.2)
1 Gy	2180 (360)	467 (124)	58.5 (1.6)	54.5 (2.1)	65.6 (1.8)
2 Gy	1870 (410)	504 (198)	59.2 (0.8)	55.6 (1.2)	65.6 (0.8)

Notes. Ps.BFR, periosteal bone formation rate; Ec.BFR, endosteal bone formation rate. Data reported as mean (SD).